

Comparative study of pulsed laser diode end-pumped thulium-doped 2-μ m Q-switched lasers

Ya Wen(温雅), Zhen Fan(范震), Lin-Hao Shang(尚林浩), Guang-Yong Jin(金光勇), Wang Chao(王超), Xin-Yu Chen(陈薪羽), and Chun-Ting Wu(吴春婷)

Citation: Chin. Phys. B, 2021, 30 (**3**): 034206. DOI: 10.1088/1674-1056/abca21
Journal homepage: http://cpb.iphy.ac.cn; http://iopscience.iop.org/cpb

What follows is a list of articles you may be interested in

Analysis of dark soliton generation in the microcavity with mode-interaction

Xin Xu(徐昕), Xueying Jin(金雪莹), Jie Cheng(程杰), Haoran Gao(高浩然), Yang Lu(陆洋), and Liandong Yu(于连栋)

Chin. Phys. B, 2021, 30 (**2**): 024210. DOI: 10.1088/1674-1056/abc3b4

Dynamic measurement of beam divergence angle of different fields of view of scanning lidar

Qing-Yan Li(李青岩), Shi-Yu Yan(闫诗雨), Bin Zhang(张斌), and Chun-Hui Wang(王春晖)

Chin. Phys. B, 2021, 30 (**2**): 024205. DOI: 10.1088/1674-1056/abc155

Synthesis of new silicene structure and its energy band properties

Wei-Qi Huang(黄伟其), Shi-Rong Liu(刘世荣), Hong-Yan Peng(彭鸿雁), Xin Li(李鑫), Zhong-Mei Huang(黄忠梅)

Chin. Phys. B, 2020, 29 (**8**): 084202. DOI: 10.1088/1674-1056/ab942c

High-performance frequency stabilization of ultraviolet diode lasers by using dichroic atomic vapor spectroscopy and transfer cavity

Danna Shen(申丹娜), Liangyu Ding(丁亮宇), Qiuxin Zhang(张球新), Chenhao Zhu(朱晨昊), Yuxin Wang(王玉欣), Wei Zhang(张威), Xiang Zhang(张翔)

Chin. Phys. B, 2020, 29 (**7**): 074210. DOI: 10.1088/1674-1056/ab8c41

575-fs passively mode-locked Yb:CaF_2 ceramic laser

Cong Wang(王聪), Qian-Qian Hao(郝倩倩), Wei-Wei Li(李威威), Hai-Jun Huang(黄海军), Shao-Zhao Wang(王绍钊), Da-Peng Jiang(姜大朋), Jie Liu(刘杰), Bing-Chu Mei(梅炳初), Liang-Bi Su(苏良碧)

Chin. Phys. B, 2020, 29 (**7**): 074205. DOI: 10.1088/1674-1056/ab8ac5

Comparative study of pulsed laser diode end-pumped thulium-doped 2-μm *Q*-switched lasers*

Ya Wen(温雅), Zhen Fan(范震), Lin-Hao Shang(尚林浩), Guang-Yong Jin(金光勇), Wang Chao(王超), Xin-Yu Chen(陈薪羽), and Chun-Ting Wu(吴春婷)†

Jilin Key Laboratory of Solid Laser Technology and Application, College of Science, Changchun University of Science and Technology, Changchun 130022, *China*

(Received 4 September 2020; revised manuscript received 20 October 2020; accepted manuscript online 13 November 2020)

We report pulsed laser diode (LD) end-pumped acoustic *Q*-switched Tm:YAG laser, Tm:LuAG laser, and Tm:LuYAG laser and the physical properties and spectra of Tm:YAG, Tm:LuAG, and Tm:LuYAG are analyzed. The Tm:LuYAG laser is pumped by 785-nm and 788-nm pulses separately, and is compared with Tm:YAG laser. Different output energy values and output wavelengths of Tm:LuAYG lasers pumped by LDs with different wavelengths are obtained and compared with each other. When the repetition frequency is 100 Hz, the pulsed Tm:YAG laser has single pulse energy of 15.9 mJ, pulse width of 126.7 ns, and the center wavelength of 2013.36 nm, and the pulsed Tm:LuAG laser possesses single pulse energy of 11.8 mJ, pulse width of 252.4 ns, and the center wavelength of 2023.65 nm, and the pulsed Tm:LuYAG laser output energy values are 12.32 mJ and 12.25 mJ with the slope efficiencies of 12.5% and 11.85%, the center wavelengths of 2017.89 nm and 2027.11 nm, respectively, while the pump sources are 785-nm and 788-nm pulsed LDs, respectively.

Keywords: thulium-doped crystal, bonded crystal, mixed crystal, 2-μm laser

PACS: 42.55.–f, 42.55.Xi, 42.60.Gd **DOI:** 10.1088/1674-1056/abca21

1. Introduction

The 2-μm lasers with small absorption in the atmospheric window and eye-safety band, which contains the absorption peaks of CO_2 and water molecules, are widely used in medical operations, laser ranging and lidar. The 2-μm lasers have good atmospheric transmission performance, which is of great significance in developing the optical communication and optical remote sensing, as well as lidar and laser communication.[1,2] The 2-μm lasers are useful pump sources for Mid-IR 3 μm–5 μm optical parametric oscillators (OPOs), which are important for expanding the 3 μm–5 μm, 8 μm–12 μm mid-and far-infrared lasers. Therefore, high efficiency, high energy, wide wavelength tuning range, and good stability are the main development direction of 2-μm lasers.[3–5]

The radiation of 2-μm wavelength is obtained practically by lasers based on the active media doped with thulium, holmium or a mixture of thulium and holmium together or by 1-μm lasers pumped OPOs or the Ho-lasers pumped by Tm-lasers. However, the process of generating 2-μm laser by OPO is complicated, which is not conducive to the development of miniaturized and integrated laser light source.[6,7] The Tm and Ho co-doped media with large emission cross section, which can meet the requirements of generating high peak power laser pulse, but they must be cooled to lower temperature, suffering more high up-conversion effects and energy transferring between Tm and Ho. However, it is difficult to obtain a 2-μm laser with large energy and high repetition rate at room temperature. Therefore, in this paper the 2-μm laser output with high-energy, high-repetition-frequency can be obtained by directly pumping single-doped Tm laser crystals with a laser diode (LD) at about 800 nm.

Tm-doped 2-μm solid-state lasers are such as Tm:YAG laser, Tm:LuAG laser, Tm:YAP laser, Tm:YLF laser, Tm:$GdVO_4$ laser, *etc*. The representative yttrium aluminum garnet (YAG, $Y_3Al_5O_{12}$) crystal of garnet crystal belongs to the cubic system, and the output band is mainly around 2013 nm–2025 nm.[8] The crystal of aluminum acid represented by yttrium aluminium oxide (YAP, $YAlO_3$) is an optical negative biaxial crystal, which belongs to the orthorhombic system, and its output band is mainly in a range of 1938 nm–1990 nm,[9] the fluoride crystal represented by yttrium lithium fluoride (YLF, Y_iLF_4) belongs to the tetragonal system, and the output band is mainly near 1900 nm.[10] The vanadate crystals represented by gadolinium vanadate ($GdVO_4$) belong to tetragonal positive uniaxial crystals, and the output band is near 1910 nm.[11] In terms of material, the output wavelength of the garnet crystal is in a range of 2013 nm–2025 nm. Compared with other substrates, YAG crystal is close to 2 μm. Therefore, this paper mainly studies the output characteristics of a single thulium-doped garnet crystal system.

The solid solution $(Lu_xY_{1-x})_3Al_5O_{12}$ series with the garnet-type structure has attracted much attention in laser applications, and the end member compound YAG ($Y_3Al_5O_{12}$) is well known, the end member compound LuAG ($Lu_3Al_5O_{12}$) is considered to be a promising material for quasi-three-level laser hosts. The Tm:YAG crystals' center wavelength

*Project supported by the National Natural Science Foundation of China (Grant Nos. 11974060 and U19A2077).

†Corresponding author. E-mail: bigsnow1@126.com

© 2021 Chinese Physical Society and IOP Publishing Ltd

is 2014 nm, the Tm:LuAG crystals' center wavelength is 2023 nm. The output wavelength of Tm:LuAG crystals deviates more from the absorption peak of water and CO_2, and is closer to the effective wavelength of lidar. One point concerning the front-end part is that the small thermal conductivity of the LuAG matrix and the thermal lens effect of Tm:LuAG crystals are more serious than those of Tm:YAG, and it is difficult to obtain larger laser output.[12] With the improvement of crystal growth technology, the $(Lu_xY_{1-x})_3AG$ series of mixed crystals is gradually applied to experimental research. The main advantage of LuYAG mixed crystal is to reduce the content of Lu_2O_3 in the matrix, the price of crystal and the freezing point temperature of LuAG grown in a crucible, to overcome the shortcomings of Tm:LuAG crystals, and to increase the content of $Y_3Al_5O_{12}$ for retaining the advantages of Tm:YAG crystals. Compared with LuAG crystals, the LuYAG crystals have a very attractive feature. When considering the center laser wavelength, the LuYAG crystals have another attractive feature compared with YAG crystals.[13]

In recent years, the Tm:LuYAG lasers have experienced a rapid development. For example, in 1994, Kmetec *et al.*[14] reported the Tm:YAG, Tm:LuAG, and Tm:LuYAG lasers. The lasers' operation by diode pumping, the pump source is 785 nm. When the pump power was about 12 W, the Tm:LuYAG laser obtained maximum output power of 3 W and a slope efficiency of 33%. At the room temperature, when the substitution concentration of Lu in YAG is 0%, 50%, and 100%, the central wavelength of laser is 2013.3 nm, 2022.7 nm, and 2020.3 nm respectively. In 2004, Kuwano *et al.*[15] successfully grew $Tm:Lu_{0.5}Y_{2.5}AG$ crystal, and the central wavelength was 2022.7 nm. Compared with 2020.3 nm of Tm:LuAG and 2013.3 nm of Tm:YAG, the wavelength of Tm:LuYAG deviates greatly from the absorption band of water and CO_2, and is very conducive to the transmission of laser in the atmosphere. In 2012,[16] Sun *et al.* reported that a 788-nm diode-pumped Tm:LuYAG was used to achieve 1935.3 nm–1994.9 nm continuous wave laser, and at 1999.7 nm they achieved 1.76-W output power, corresponding to a slope efficiency of 21.41%. In 2016, Zhao *et al.*[17] reported a 785-nm pumped Tm:LuYAG laser. Under continuous operation, the maximum output power was 3.05 W, the ramp efficiency was about 33%, and when the acoustic-optic Q-switched repetition frequency was 500 Hz, the maximum single pulse energy was 1.4 mJ, and the center wavelength was 2.02 μm.

It can be seen that Tm:LuYAG can be pumped by a variety of pump sources, and the use of different pump sources has a great influence on its output wavelength and characteristics. From the point of view of laser technology, the mixed crystal generally has a wider absorption and emission spectrum than the end member compound crystal. For the application of long-distance lidar remote sensing with eye safety, 2-μm coherent lidar is the best matching wavelength, and the corresponding window wavelengths are 2065.48 nm and 2091.28 nm, respectively. And the closer to 2.1 μm the matching wavelength, the smaller the absorption coefficient of atmospheric molecules, the weaker the signal attenuation, and the advantageous the lidar remote sensing technology will be. Due to the limitation of the output wavelengths of Tm:YAG laser and Tm:LuYAG laser, the hybrid crystal Tm:LuYAG is expected.

There are few reports on Tm:LuYAG crystal, and the Q-switched Tm:LuYAG laser output characteristics of pulsed pump have not been reported. In this paper, we use 785-nm and 788-nm pulsed pump sources to pump Q-switched Tm:LuYAG laser, and compare it with the pulsed Tm:YAG laser and Tm:LuAG laser. We evaluate the output characteristics of Tm:YAG, Tm:LuAG, and Tm:LuYAG gain media at a wavelength of 2 μm.

2. Physical properties and spectra of Tm:YAG, Tm:LuAG, and Tm:LuYAG

In Tm^{3+} metal ions, the phonon broadening of 4f electrons and the multiplicity of Stark energy levels provide the tunability ability near 2 μm. The wavelength of 785 nm emitted by high power GaAlAs laser diode is used to pump the Tm^{3+}-doped crystal. The 785-nm pumping radiation transfers the Tm^{3+} from the $^3H_6$ ground state to the $^3H_4$ level. The ion transits from the $^3H_4$ pump level to the upper level $^3F_4$ via relaxation oscillation. The laser interaction takes place between the $^3F_4$ level and the lower laser level of the $^3H_6$ ground state multiple terahertz, and the wavelength of the output radiation is around 2 μm.[18,19]

When choosing the matrix doped with metal ions, it is necessary to ensure that the lattice position of the matrix crystal can accommodate the doped ions, and its local crystal field must have symmetry and the intensity necessary for sensing the desired spectral characteristics. The optical properties of the crystal after doping metal ions should be considered. The change of refractive index will lead to the uneven propagation of light in the crystal, resulting in poor beam quality, the mechanical and thermal properties of the matrix will affect the average power of the crystal, the thermal conductivity, hardness and crack resistance will affect the heat dissipation of the crystal to withstand the energy.

The refractive index of laser crystal can be calculated by Sellmeiyer relation[20]

$$n(\lambda)^2 - 1 = \frac{A_1\lambda^2}{\lambda^2 - B_1} + \frac{A_2\lambda^2}{\lambda^2 - B_2} + \frac{A_3\lambda^2}{\lambda^2 - B_3}, \tag{1}$$

where n is the refractive index of the laser crystal, λ is the output wavelength, A_1, A_2, A_3, B_1, B_2, and B_3 are the Sellmeiyer constants, and the Sellmeiyer constants for YAG, LuAG, and LuYAG are shown in Table 1.[15] The ratio of Lu atom to Y atom in Tm:LuYAG is 1:1.

Table 1. Sellmeiyer constants of YAG, LuAG, and LuYAG.

	A_1	A_2	A_3	B_1	B_2	B_3
YAG	1.28040	1.00244	4.57401	5.49568×10^{-3}	1.92189×10^{-2}	3.87058×10^{2}
LuAG	1.47119	8.45642×10^{-1}	3.82124	6.21359×10^{-3}	2.00432×10^{-2}	3.30483×10^{2}
LuYAG	1.77362	5.27323×10^{-1}	3.87734	7.90836×10^{-3}	2.31844×10^{-2}	3.32469×10^{2}

According to the Sellmeiyer relation, the peak refractive index of Tm:YAG crystals is about 1.8 in a range of 2.0 μm–2.1 μm, that of Tm:LuAG crystals is about 1.81 in a range of 2.0 μm–2.1 μm, and that of Tm:LuYAG crystals is about 1.805 in a range of 2.0 μm–2.1 μm.

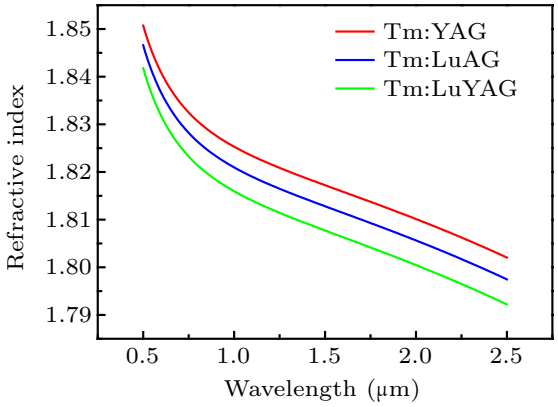


Fig. 1. Curves of refractive index versus wavelength of YAG, LuAG, and LuYAG crystal.

For lasers, the gain cross section of the laser medium can be estimated by the cross section of the laser medium, and the gain of the laser is judged accordingly. The absorption coefficient of the crystal can be expressed as[20]

$$\alpha(\lambda) = \frac{1}{l}\cdot\left\{2\times\ln\left[1-\left(\frac{n-1}{n+1}\right)^2\right] + \ln\left[1+\left(\frac{n-1}{n+1}\right)^4\right] - \ln(T)\right\}, \quad (2)$$

where l is the length of crystal, n is the refractive index of crystal, and T is the transmittance of crystal to pump light.

The absorption cross section expression of laser medium is[21]

$$\sigma_{\text{abs}} = \alpha/N, \quad (3)$$

where N is the number of Tm^{3+} ions in unit volume. We are most concerned about the number of particles that transit at $^3H_6$–$^3H_4$ when the absorption peak is 785 nm. The doping concentration of the Tm:YAG, Tm:LuAG, and Tm:LuYAG crystals used in the calculation and measurement are the same as the concentration used in the experiment, specifically, both are 3.5%.

The fluorescence spectra of Tm:YAG, Tm:LuAG, and Tm:LuYAG crystal are measured under the action of pump light source as shown in Fig. 2.

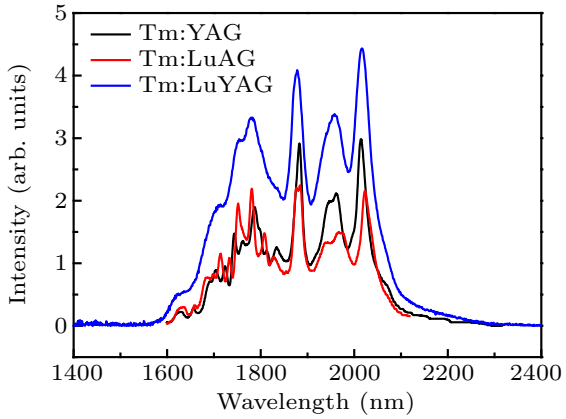


Fig. 2. Fluorescence spectrum of Tm:YAG, Tm:LuAG, and Tm:LuYAG.

The study of the fluorescence spectrum of the single doped Tm^{3+} laser medium is mainly about the transition of the Tm^{3+}:$^3F_4 \rightarrow {}^3H_6$ level.[22] The emission wavelength is in a range of 1800 nm–2100 nm. The energy level splitting[23] is shown in Fig. 3.

The fluorescence spectra of Tm:YAG, Tm:LuAG, and Tm:LuYAG crystal in the range of 1800 nm–2100 nm are very similar to each other. The central wavelength of fluorescence spectrum of Tm:YAG crystal is 2014 nm in a range of 2006 nm–2024 nm, the central wavelength of fluorescence spectrum of Tm:LuAG crystals is 2023 nm in a range of 2015 nm–2035 nm, and the central wavelength of fluorescence spectrum of Tm:LuYAG crystals is 2019 nm in a range of 2000 nm–2033 nm. It can be seen that the emission wavelength of Tm:LuAG crystals is closer to the atmospheric window, far from the absorption peaks of carbon dioxide and water. The spectrum of Tm:LuYAG crystals is related to the mixing ratio of Lu_2O_3 to $Y_3Al_5O_{12}$. It can be seen that the changing of the mixing ratio of Lu atom to Y atom has a great influence on the fluorescence emission wavelength of the crystal. There are few reports on the laser based on Tm:LuYAG crystals as the working material, and the performance evaluation is not comprehensive. However, in view of its huge potential in crystal growth cost and laser output performance, in this paper Tm:YAG and Tm:LuAG, the isomorphic crystals of Tm:LuYAG are used as the working materials to carry out the experimental research on them, and the output characteristics of the three kinds of crystals in the 2-μm band are compared and analyzed.

The physical properties of Tm:YAG, Tm:LuAG, and Tm:LuYAG are shown in Table 2.

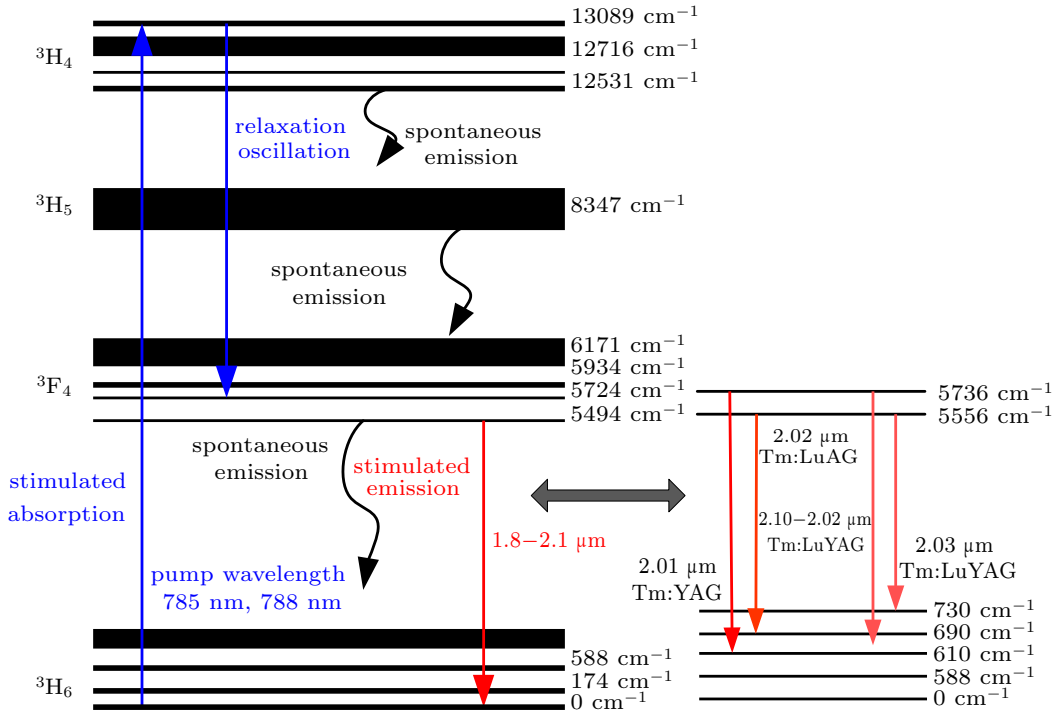


Fig. 3. Energy level diagram of Tm^{3+} lasers.

Table 2. Physical properties of Tm:YAG, Tm:LuAG, and Tm:LuYAG laser crystal.

Crystal	Tm:YAG	Tm:LuAG	Tm:LuYAG
Chemical formula	Tm:$Y_3Al_5O_{12}$	Tm:$Lu_3Al_5O_{12}$	Tm:$Lu_{1.5}Y_{1.5}Al_5O_{12}$
Crystal system	cubic system	cubic system	cubic system
Density (g/cm^3)	4.56	6.32	5.64
Thermal conductivity (W/(cm· K))	0.13	0.079	0.075
Thermal expansion coefficient (10^{-6} K)	7.8∼8.5	7.9	8.0
Melting point (K)	∼ 2220	∼ 2000	∼ 2320
Fluorescence lifetime (ms)	13.9	11.7	9∼11
Absorption cross section (10^{-21} cm^2)	6.5	5.4	5.716
Stimulated emission cross section (10^{-21} cm^2)	2.5	1.4	1.4

Different matrix provides different crystal field for Tm^{3+} and also affects the spectral parameters of the crystal. It is reported that the tuning range of 135 nm from 1938 nm to 2073 nm is achieved from Tm:YAG laser, and the tuning range of 95 nm from 1966 nm to 2061 nm is acquired from Tm:LuAG laser,[14] and the tuning range of 187 nm from 1935.3 nm to 2123.2 nm is obtained from Tm:LuAG laser.[9] Although the wavelength increase of Tm:LuYAG lasers is very small, it has a very important influence on the application of laser. The increase of wavelength greatly reduces the absorption of H_2O and CO_2 in the atmosphere. Therefore, it is necessary to comparative analysis of the Tm:YAG, Tm:LuAG, and Tm:LuYAG lasers output characteristics, which can be selected in practical applications.

3. Laser experiments

In this experiment, two kinds of pump sources are used,. One type is NL-P4-60-0788, the fiber-coupled LD module can provide 60-W CW power with are petition frequency of 10 Hz–1 kHz, and the pulse width adjustment range is 1 ms–100 ms. The fiber diameter is 400 μm and a numerical aperture is 0.22. The central wavelength of the LD is 785 nm, with the air cooling temperature being 22 °C. The other type is WPL-788 nm–70 W, the fiber-coupled LD module can provide 70-W CW power with a repetition frequency of 100 Hz–1 kHz and a pulse width adjustment range of 1 ms–10 ms. The fiber diameter is 400 μm and a numerical aperture is 0.22. The central wavelength of the LD is 788 nm with a cooling water temperature of 20 °C. Two pulsed LDs double-end-pump the Tm^{3+}

crystals at the same time. The Tm^{3+} crystals are in the state of being pumped and stopped at the same time. The Tm^{3+} crystal laser cavity configuration is shown in Fig. 4.

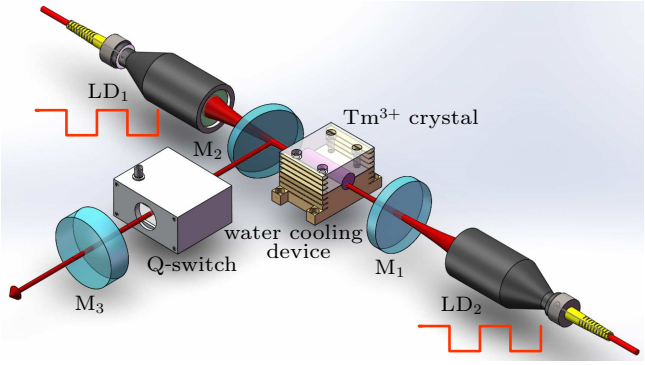


Fig. 4. Schematic diagram of experimental setup.

The pump beam is shaped by a beam integration system, and the pump waist of 800 μm in diameter is positioned on the crystal. The gain media are Tm:YAG, Tm:LuAG, and Tm:LuYAG laser rods, respectively, with doped YAG, LuAG and LuYAG double end caps with the same Tm^{3+} doping concentration of 3.5%, the same rod diameter of 3 mm and the same doping length of 15 mm, and the same non-doped length of 5 mm. Each end face of the Tm:YAG crystals is of antireflection coated at the pump (785 nm) and laser wavelength (2000 nm–2050 m). Each end face of the Tm:LuAG crystals is of antireflection coated at the pump (788 nm) and laser wavelength (2000 nm–2100 nm). Each end face of the Tm:LuYAG crystals is of antireflection coated at the pump (785 nm–810 nm) and laser wavelength (2000 nm–2100 nm). Few researches on Tm:LuYAG crystals show that the crystals are coated with a wide antireflection membrane. In this paper, the output characteristics of Tm:LuYAG crystals prepared by two pump sources will be compared and analyzed.

The water-cooled acousto-optic Q-switch produced by British Gooch Company is selected as an acousto-optic Q-switch system. Q-switch type is QS041-10M-HI8. The Q-switching crystal is a quartz crystal with 2 cm in light diameter and 46 mm in length, and its RF power is 40.68 MHz, driving mode: MQH041-50DM-A05.

Pulsed LD double end pumped L-shaped acoustic-optic Q-switched Tm^{3+} lasers are used in this experiment. The pulsed LD duty ratios are all 50% and the repetition frequencies are 100 Hz, 200 Hz, and 500 Hz. In the experiment, pulsed LD double end pumping is used. The repetition frequency of LD is 100 Hz and the duty cycle is 50%. Using one plano-concave resonator, the cavity length is 120 mm. High reflectivity mirror (HR) M_1 is broadband high reflected plane mirror in a range from nearly 2.0 μm to 2.1 μm ($R > 99.5\%$), antireflection coated at 785 nm–808 nm ($R < 0.5\%$); M_2 is 45° angle-of-incidence dichroic fold mirror with high transmittance (HT) coated at 785 nm–808 nm ($T > 99\%$) and HR coated at 2.0 μm–2.1 μm ($R > 99.5\%$). The output coupler (OC) M_3 is coated at 2.0 μm–2.1 μm with the reflectivity of 96%, the plane-concave lens has a radius of curvature of 150 mm.

In the experiments, the output power is measured by an F150A-BB-26 power meter (Ophir Photonics). A high-speed silicon photodiode (PCT-3TE-12,Vigo Inc.) is used to detecte Q-switched laser pulse and a digital oscilloscope (DPO3054, Tektronix Inc.) is used to record the pulse signal. The laser spectrum is measured by an optical spectrum analyzer (AQ6357, Yokogawa) with a resolution of 0.05 nm.

4. Experimental results and discussion

The 785-nm pulsed LD and 788-nm pulsed LD are used as the pumping sources to pump Tm:YAG laser and Tm:LuAG Q-switched laser, respectively. The 785-nm and 788-nm pulsed LDs are used to pump Q-switched Tm:LuYAG laser separately. The experimental results of the average power, pulse width and center wavelength of the laser output are obtained when the Q-switched repetition frequencies are 100 Hz, 200 Hz, and 500 Hz, respectively.

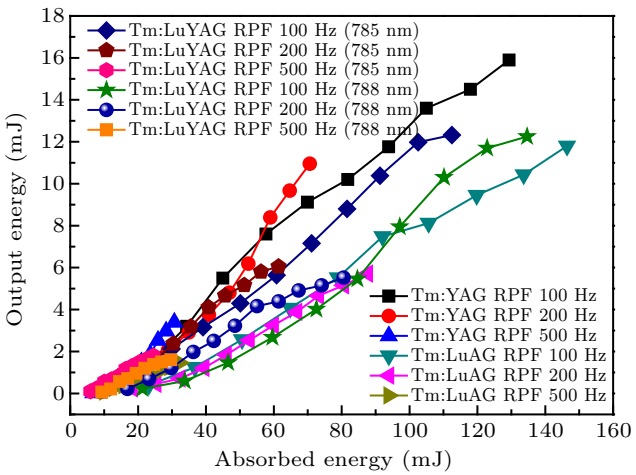


Fig. 5. Variations of the output energy with the pump energy of Tm:YAG, Tm:LuAG, and Tm:LuYAG lasers at different repetition rates.

Figure 5 shows the variations of output energy with pump energy of Tm:YAG, Tm:LuAG, and Tm:LuYAG lasers at different repetition rates and different pump sources. Table 3 summarizes the laser parameters of the investigated Tm:YAG, Tm:LuAG, and Tm:LuYAG crystals.

It can be seen from Fig. 5 and Table 3 that with the increase of repetition rate, the maximum pump energy, and output energy of the crystal decrease gradually. When the laser operates at the best repetition frequency, the efficiency of the crystal will be highest, and it is possible to obtain larger energy. The high energy level lifetime of Tm:YAG and Tm:LuAG crystals (13.9 ms, 11.7 ms) determine that the best repetition rate of the laser is around 100 Hz, which makes it difficult to achieve an output with high repetition rate. The emission cross-section of Tm:LuAG crystal is small, which

leads to a low gain, low energy extraction efficiency, and serious thermal effect. The *Q*-switched Tm:LuAG laser output properties are worse than those of the *Q*-switched Tm:YAG laser.

Compared with the Tm:LuAG and Tm:LuYAG crystals, the Tm:YAG crystal is very suitable for high energy laser output, which possesses a larger absorption cross-section (6.5×10^{-21} cm^2) at pumping wavelength, a larger gain cross section (2.5×10^{-21} cm^2) and a larger thermal conductivity (0.13 W/(cm·K)). While, the absorption cross-section of Tm:LuAG crystals is 5.4×10^{-21} cm^2, the gain cross section is1.4×10^{-21} cm^2, and the thermal conductivity is 0.079 W/(cm·K). And for the Tm:LuYAG crystals, the absorption cross-section is 5.716×10^{-21} cm^2, the gain cross section is 1.4×10^{-21} cm^2, and the thermal conductivity is 0.075 W/(cm·K). Because Tm:LuAG and Tm:LuYAG crystals have similar optical and thermal properties, and their output energy values and efficiencies are close.

Table 3. Laser parameters of investigated Tm:YAG, Tm:LuAG, and Tm:LuYAG crystals.

Crystals	LD (nm)	RPF (Hz)	Threshold energy (mJ)	Max. output (mJ)	Slope eff. (%)
Tm:YAG	785	100	10.28	15.9	13.52
		200	10.87	10.95	18.37
		500	6.86	3.39	14.15
Tm:LuAG	788	100	23.17	11.8	9.5
		200	18.36	5.12	8.01
		500	10.13	1.464	6.22
Tm:LuYAG	785	100	8.94	12.32	12.5
		200	9.46	6.05	12.39
		500	5.97	1.804	9.36
Tm:LuYAG	788	100	21.3	12.25	11.85
		200	16.88	5.52	8.88
		500	9.31	1.606	8.07

Figure 6 shows a multiple pulse train of 788-nm LD pumped acoustic–optic *Q*-switched Tm:LuYAG laser pulses at 100 Hz. The *Q*-switched operation is quite stable and the power jitter is less than 2.5%.

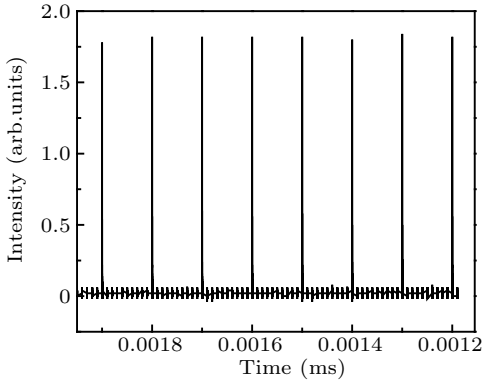


Fig. 6. Pulse train of 788-nm LD pumped acoustic–optic *Q*-switched Tm:LuYAG laser.

Figure 7 shows the variation of Tm:YAG, Tm:LuAG, and Tm:LuYAG laser pulse widths with output energy at a repetition rate of 100 Hz, showing that with the output energy increasing, the pulse width becomes narrow and tends to a stable value. This approximate stable value is determined by the lifetime of the photon in the cavity. The pulse width and peak power at the maximum output energy are shown in Table 4.

The pulsed Tm:YAG laser obtains a maximum single pulse energy value and the narrowest pulse width. The single pulse energy obtained by the pulse Tm:LuYAG laser is higher than that of the pulse Tm:LuAG laser and lower than that of the pulse Tm:YAG laser, the pulse width is slightly larger than that of the pulse Tm:LuYAG laser and wider than that of the pulse Tm:YAG laser. Under the same conditions, the larger the cross-section of gain of laser medium, the narrower the output pulse width will be.

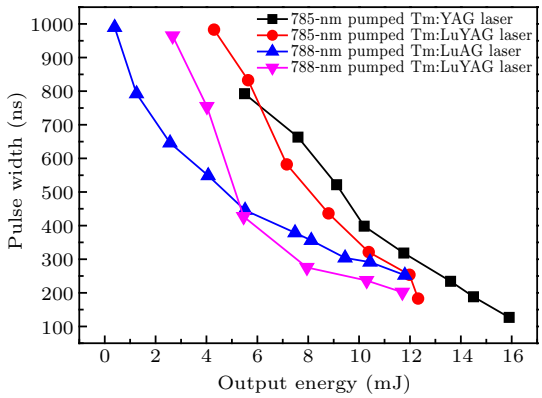


Fig. 7. Variations of output pulse width with output energy of Tm:YAG, Tm:LuAG, and Tm:LuYAG lasers.

Table 4. Parameters of pulse width and peak power of Tm:YAG, Tm:LuAG, and Tm:LuYAG laser.

Crystals	LD (nm)	RPF (Hz)	Pulse width (ns)	Peak power (kW)
Tm:YAG	785	100	126.7	125.49
Tm:LuAG	788	100	252.4	46.75
Tm:LuYAG	785	100	182.7	67.43
Tm:LuYAG	788	100	201.7	60.73

Figure 8 shows the Tm:YAG, Tm:LuAG, and Tm:LuYAG laser's central wavelengths at a repetition rate of 100 Hz with

the single pulse energy being minimum. The pulsed Tm:YAG laser wavelength is centered at 2013.36 nm, and the pulsed Tm: LuAG laser wavelength is centered at 2023.65 nm. The absorption peak of Tm:LuYAG is at 785 nm, and the pulsed laser output wavelength is centered at 2017.89 nm. For the absorption peak of Tm:LuYAG at 788 nm, the pulsed laser output wavelength is centered at 2027.11 nm.

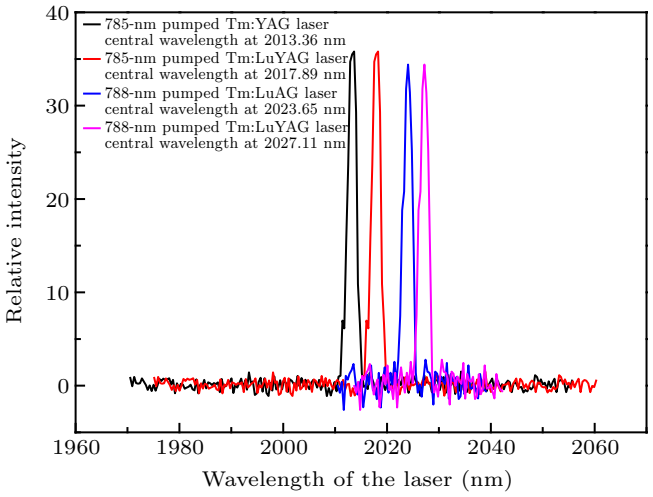


Fig. 8. Output spectra of Tm:YAG, Tm:LuAG, and Tm:LuYAG lasers.

From Fig. 3 it follows that the laser radiation at 2 μm takes place between the lower level of $^3F_4$ and the higher level of $^3H_6$, including 610 cm^{-1} and 730 cm^{-1}.[23] When the central wavelengths of the pump are 785 nm and 788 nm, the ions transit from the lowest Stark sub-level in $^3F_4$ at 5736 cm^{-1} and 5556 cm^{-1} to $^3H_6$ level, resulting in the possible laser emissions at 2.01 μm–2.02 μm and 2.02 μm, respectively. The results show that different output central wavelengths can be achieved under different pumping wavelengths.

5. Conclusions

In this work, we demonstrate pulsed LD end-pumped pulsed Tm:YAG, Tm:LuAG, and Tm:LuYAG lasers. When using the 785-nm pulsed LD with a repetition frequency of 100 Hz, the single pulse energy of 15.9 mJ is obtained for pulsed Tm:YAG laser and 12.32 mJ is obtained for pulsed Tm:LuYAG laser. When using the 788-nm pulsed LD with a repetition frequency of 100 Hz, the single pulse energy of 11.8 mJ is obtained for the pulsed Tm:LuAG laser and 12.25 mJ is obtained for the pulsed Tm:LuYAG laser. The center wavelengths of Tm:LuYAG laser are 2017.89 nm and 2027.11 nm, when the pump sources are 785 nm and 788 nm in wavelength, respectively. The experimental results show that the doped Tm:LuYAG crystal has a wide absorption band, and the output wavelength is longer than that of Tm:YAG crystal, and the efficiency is equivalent to that of Tm:LuAG crystal. For the end member compound crystals, the Tm:LuYAG mixed crystals have higher research significance and practical application value.

References

[1] Liu X Y, Li X W, Zhao S Z, Yang K J, Guo L, Li T, Qiao W C, Li M, Zhang B T, He J L, Zheng L H, Su L B and Xu J 2019 *Chin. Opt. Lett.* **17** 091401
[2] Liu X, Huang H T, Zhu H Y, Shen D Y, Zhang J and Tang D Y 2015 *Chin. Opt. Lett.* **13** 061404
[3] Liu X L, Huang H T, Shen D Y, Liu X, Zhang J and Tang D Y 2014 *Chin. Opt. Lett.* **12** S21404
[4] Xie X B, Zhu X L, Li S G, Ma X H, Chen X, Sun Y G, Zang H G, Liu J Q and Chen W B 2017 *Chin. Opt. Lett.* **15** 091902
[5] Dai T Y, Deng Y, Ju Y L, Duan X M, Yao B Q and Wang Y S 2014 *Chin. Phys. Lett.* **31** 084203
[6] Yao B Q, Yu X, Ju Y L, Liu W B, Jiang B X and Pan Y B 2013 *Chin. Phys. Lett.* **30** 024210
[7] Ma Q L, Zong N, Xie S Y, Yang F, Guo Y D, Xu J L, Bo Y, Peng Q J, Cui D F and Xu Z Y 2009 *Chin. Phys. Lett.* **26** 124211
[8] Yao B Q, Ke L, Duan X M, Li G, Yang X T, Ju Y L and Wang Y Z 2009 *Phys. Lett.* **8** 563
[9] Lisiecki R, Solarz P, Dominiak-Dzik G and Ryba-Romanowski W 2006 *Phys. Rev.* **74** 035103
[10] Yu J R, Singh U N, Barnes N P and Petros M 1998 *Opt. Lett.* **10** 780
[11] Mahalingam V, Samanta T and Parveen A E 2018 *J. Matem. C* **10** 1039
[12] Suni P J M and Henderson S W 1991 *Opt. Lett.* **16** 817
[13] Pinto J F, Esterowitz L and Rosenblatt G H 1992 *Opt. Lett.* **17** 731
[14] Kmetec J D, Kubo T S, Kane T J and Grund C J 1994 *Opt. Lett.* **3** 186
[15] Kuwano Y, Suda K, Ishizawa N and Yamada T 2004 *J Cryst. Growth* **1** 159
[16] Sun M, Long J Y, Li X H, Liu Y, Ma H F, An Y, Hu X H, Wang Y S, Li C and Shen D Y 2012 *Laser Phys. Lett.* **8** 553
[17] Zhao Y G, Zhou W, Xu X D and Shen D Y 2016 *Opt. Mater.* **62** 701
[18] Zhang Q L, Feng B H, Zhang D X, Fu P M, Zhao Z W, Deng P H, Xu J, Xu Q D, Wang Y G and Ma X Y 2004 *Opt. Commun.* **232** 353
[19] Liu X, Huang H T, Zhu H Y, Shen D Y, Zhang J and Tang D Y 2015 *Chin. Opt. Lett.* **13** 061404
[20] Buryy O A, Sugak D Y, Ubizskii S B, Izhnin I I, Vakiv M M and Solskii I M 2007 *Appl. Phys B-Lasers O* **3** 433
[21] Scholle K, Heumann E and Huber G 2004 *Laser Phys. Lett.* **1** 285
[22] Li Y F, Wang Y Z and Ju Y L 2008 *Laser Phys.* **6** 722
[23] Eichhner W 2008 *Appl. Phys. B* **93** 269